Instability In Magnetic Mirror Configuration

Hunt Feng

June 14, 2023

Contents

Chapter 1

Introduction

1.1 Flow in Magnetic Nozzle

1.1.1 Magnetic Nozzle

A magnetic nozzle is a device that uses a magnetic field to shape and control the flow of charged particles in a plasma propulsion system, see Fig.1.1. By employing the magnetic mirror configuration, the magnetic nozzle can effciently direct and accelerate the plasma flow, generating thrust for propulsion. The magnetic field in the nozzle helps collimate and focus the plasma exhast, increasing its velocity and enhancing the performance of the propulsion system.

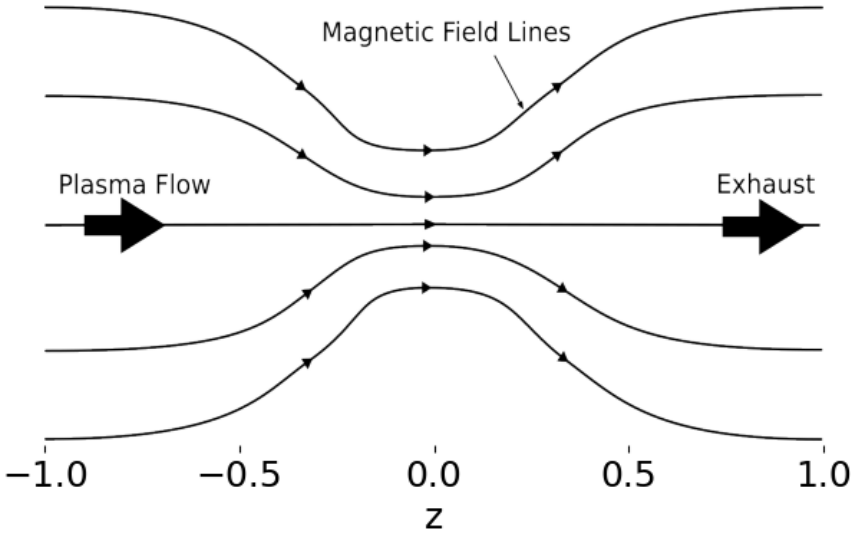

Figure 1.1: A simplified model of the magnetic nozzle

1.1.2 Magnetic Field in Magnetic Nozzle

In 1D problem, the magnetic field can be modeled as

$$B(z) = B_0 \left[1 + R \exp\left(-\left(\frac{x}{\delta}\right)^2\right)\right]$$

where $1 + R$ is the magnetic mirror ratio, and δ determines the spread of the magnetic field. It is shown in Fig.(1.2).

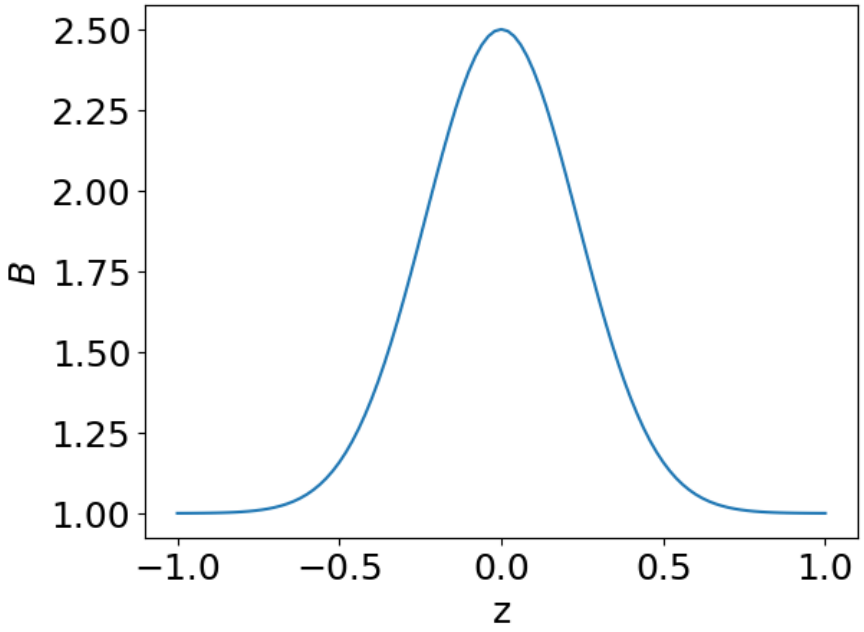

Figure 1.2: This is the magnetic field in nozzle with mirror ratio $1 + R = B_{max}/B_{min} = 2.5$, and the spread of magnetic field, $\delta = 0.1/0.3 = 0.\bar{3}$.

1.1.3 Velocity Profile at Equilibrium

Let n_0 and v_0 be the density and velocity at equilibrium (stationary solution), we know that $\partial n_0/\partial t = 0$ and $\partial v_0/\partial t = 0$, therefore n_0 and v_0 satisfy the so-called equilibrium condition,

$$\frac{\partial}{\partial z}\left(\frac{n_0 v_0}{B}\right) = 0$$
$$v_0 \frac{\partial v_0}{\partial z} = -c_s^2 \frac{1}{n_0}\frac{\partial n_0}{\partial z}$$

Let $M(z) = v_0(z)/c_s$ be the mach number (nondimensionalized velocity). The equations of motion become

$$B\frac{\partial}{\partial z}\left(\frac{n_0 M}{B}\right) = 0$$
$$M\frac{\partial M}{\partial z} = -\frac{1}{n_0}\frac{\partial n_0}{\partial z}$$

Substitute $\frac{1}{n_0}\,\partial n_0/\partial z$ using first equation, the conservation of momentum becomes

$$(M^2 - 1)\frac{\partial M}{\partial z} = -\frac{M}{B}\frac{\partial B}{\partial z}$$

Notice that there is a singularity at $M = 1$, the sonic speed.

This is a separable equation, integrate it and use the conditions at midpoint $B(0) = B_m, M(0) = M_m$ we get

$$M^2 e^{-M^2} = \frac{B^2}{B_m^2} M_m^2 e^{-M_m^2}$$

We can now express M using the Lambert W function,

$$M(z) = \left[-W_k\left(-\frac{B(z)^2}{B_m^2} M_m^2 e^{-M_m^2}\right)\right]^{1/2}$$

where the subscript k of W stands for branch of Lambert W function. When $k = 0$, it is the subsonic branch; When $k = -1$, it is the supersonic branch. Below shows a few cases of the solution.

- $M_m < 1, k = 0$, subsonic velocity profile.
- $M_m = 1$, $k = 0$ for $x < 0$ and $k = -1$ for $x > 0$, accelerating profile
- $M_m = 1$, $k = -1$ for $x < 0$ and $k = 0$ for $x > 0$, decelerating profile
- $M_m > 1, k = -1$, supersonic velocity profile

Fig.(1.3) shows some cases of the solution.

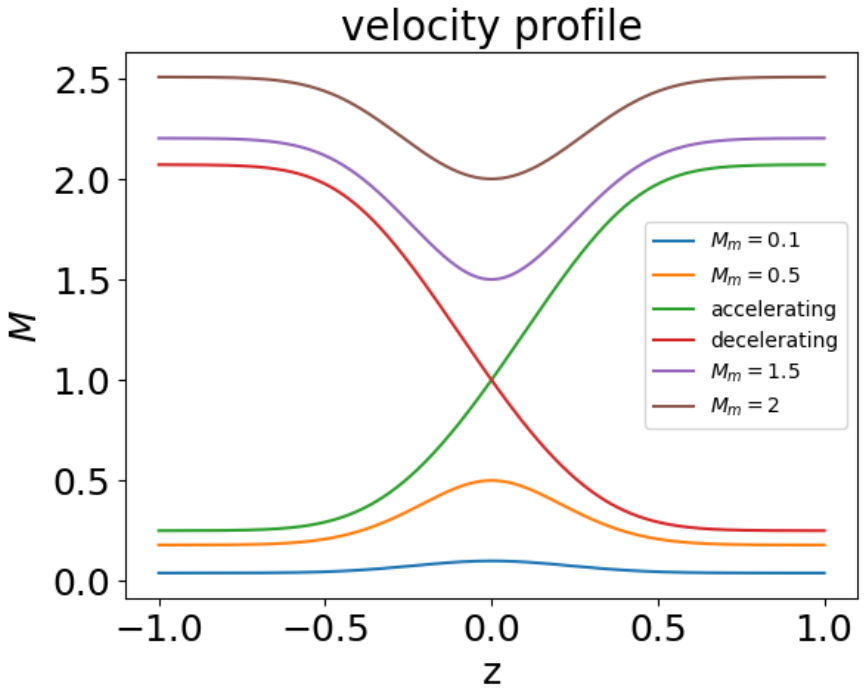

Figure 1.3: The velocity profile in the magnetic nozzle is completely determined by M_m, the velocity at the midpoint, $z = 0$. For the transonic velocity profiles, M_m alone is not enough to determine the profile, we need to specify the branch of Lambert W function to determine whether it is accelerating or decelerating.

1.1.4 Flow in Similar Configuration: Bondi-Parker Flow

Bondi derived a steady-state solution for accretion flow which is governed by Bernoulli's equation in sperical symmetry around a point mass in 1952. Then Parker solved a similar problem but with outward wind in 1958. [1, 2, 5] The equilibrium velocity profiles in such configuration are shown in Fig.1.4.

Solar wind is an example of Bondi-Parker flow. The solar wind is a stream of charged particles, primarily electrons and protons, flowing outward from the Sun.

1.2 Instability of Plasma Flow

In this section, plasma instability will be introduced and from that we will discuss the importance of this research.

The instability of plasma flow refers to the tendency of a plasma system to deviate from a stable, equilibrium state and exhibit perturbations or fluctuations in its behavior. These instabilities can arise from various factors, such as the interaction of particles with electromagnetic fields, collective effects, or the presence of gradients in plasma parameters.

Plasma flow in magnetic mirror configurations have been studied extensively in plasma physics due to its frequent precense in many areas such as the accretion flow [4, 1], and magnetic nozzle[6]. However, the stability of these configurations remains a debatable subject.

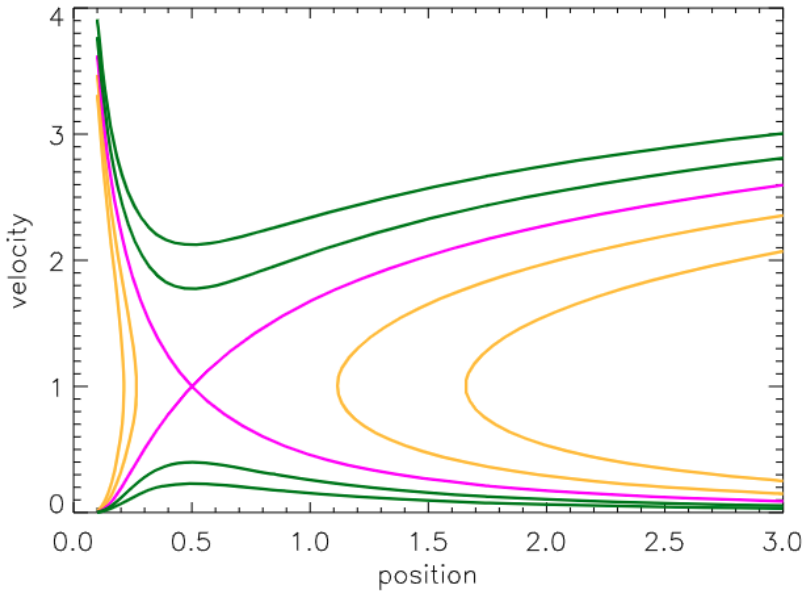

Figure 1.4: Representative trajectories of the steady-state BP flow in non-dimensional units. [5] The upward pink line represents a outward wind, it accelerates from subsonic to supersonic. The downward pink line represents an accretion flow, it accelerates towards the mass point. The green lines below the pink lines represent subsonic flows, and the green lines above represent supersonic flows. Orange lines are physically impossible scenarios.

1.3 Goal of this Thesis

The goal of this thesis is to study the instabilities of the magnetic mirror configuration given certain boundary conditions and equilibrium velocity profiles.

To achieve the goal, first we need to study the spectral method for solving the instability problem. To use spectral method, it is necessary to understand different discretizations of the operators, such as finite difference, finite element and spectral element method.

Once the spectral method is introduced, we can use it to study the instability of plasma flow in magnetic nozzle as an eigenvalue problem. We can obtain results by using different discretization techniques. By comparing the results from different approach, we can increase the credibility of the true solution.

However, spectral method is not suitable when the equilibrium velocity profile is transonic due to the precense of singularity at the sonic point. We need to solve the singular perturbation problem around the singularity analytically. Then starting from the singular point, we can use shooting method to find eigenvalues.

1.4 Outline of the thesis

The thesis will be divided into several chapters. In chapter 2, spectral method will be introduced. Chapter 3 will focus on the physics of flow in magnetic mirror configuration and derive the governing equations for charged particles, the linearized equations of motions. Following this, we will analyze the problem analytically in chapter 4. Moving to chapter 5, numerical experiments will be conducted. The conclusion will be made in chapter 6.

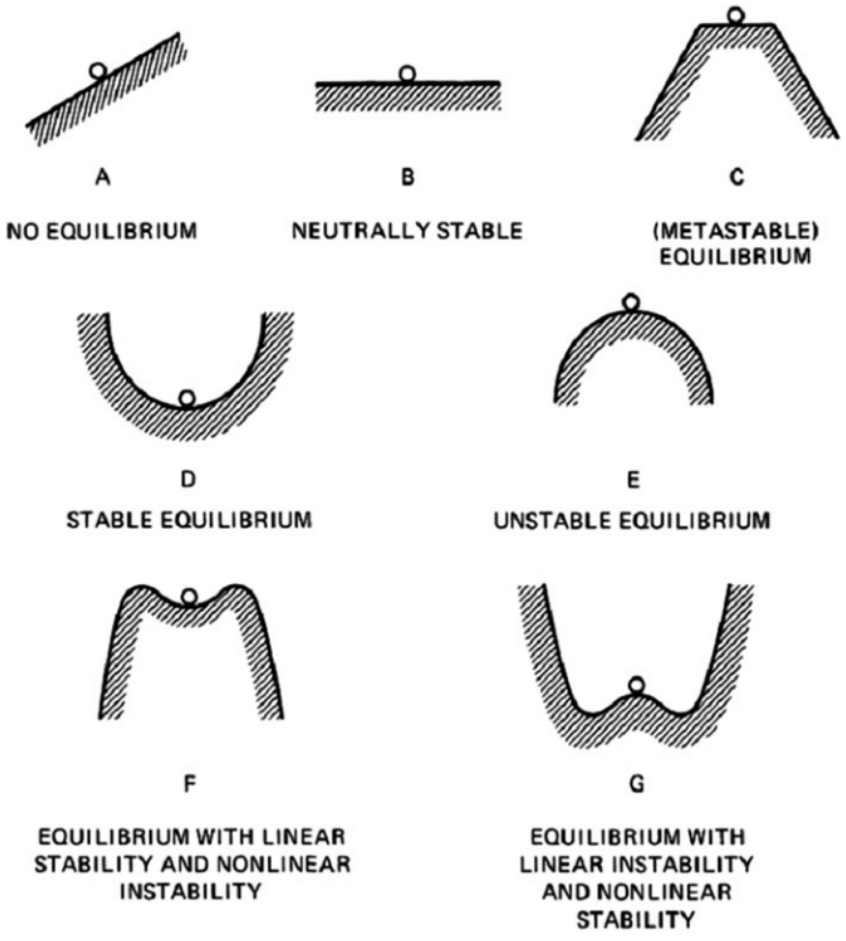

Figure 1.5: Mechanical analogy of various types of equilibrium. [3]

Chapter 2

Governing Equations

2.1 Governing Equations for Flow in Magnetic Nozzle

In this section, we will derive the governing equations of the flow in magnetic nozzle, starting from the fluid description for plasma.

In magnetic nozzle, the magnetic field is along the nozzle, which we denote as z-axis. Due to Lorentz force, the charged particles gyrates about the magnetic field lines. Because the magnetic moment is invariant in such situation (**reference**). The fluid velocity of particles can be written as $\mathbf{v} = v\mathbf{B}/B$, meaning that the particles move along the magnetic field lines. Therefore the conservation of density

$$\frac{\partial n}{\partial t} + \boldsymbol{\nabla} \cdot (n\mathbf{v}) = 0 \Rightarrow \frac{\partial n}{\partial t} + B\frac{\partial}{\partial z}\Big(\frac{nv}{B}\Big) = 0$$

In the derivation, $\boldsymbol{\nabla} \cdot \mathbf{B} = 0$ is used.

To derive the second governing equation, we start from the conservation of momentum,

$$\frac{\partial v}{\partial t} + v\frac{\partial v}{\partial z} = -\frac{1}{\rho}\boldsymbol{\nabla} p$$

Let $\boldsymbol{\nabla} p = k_B T\ \partial n/\partial z$, we have

$$\frac{\partial v}{\partial t} + v\frac{\partial v}{\partial z} = -c_s^2\frac{1}{n}\frac{\partial n}{\partial z}$$

where $c_s^2 = k_B T/m$ is the square of sound speed.

Therefore the dynamics of the flow in magnetic nozzle can be characterized by the conservation of density and momentum,

$$\frac{\partial n}{\partial t} + B\frac{\partial}{\partial z}\Big(\frac{nv}{B}\Big) = 0$$
$$\frac{\partial v}{\partial t} + v\frac{\partial v}{\partial z} = -c_s^2\frac{1}{n}\frac{\partial n}{\partial z}$$

2.2 Linearized Equations

For convenience, we nondimensionalize the governing equations by normalizing the velocity to c_s, $v \mapsto v/c_s$, z to system length L, $z \mapsto z/L$ and time $t \mapsto c_s t/L$. The governing equations become

$$\frac{\partial n}{\partial t} + n\frac{\partial v}{\partial z} + v\frac{\partial n}{\partial z} - nv\frac{\partial_z B}{B} = 0 \tag{2.1}$$
$$n\frac{\partial v}{\partial t} + nv\frac{\partial v}{\partial z} = -\frac{\partial n}{\partial z} \tag{2.2}$$

and the nondimensionalized equilibrium condition is

$$\frac{\partial}{\partial z}\left(\frac{n_0 v_0}{B}\right) = 0 \tag{2.3}$$

$$v_0 \frac{\partial v_0}{\partial z} = -\frac{1}{n_0}\frac{\partial n_0}{\partial z} \tag{2.4}$$

Now we are going to derive an important intermediate result, the linearized governing equations. Let $n = n_0(z) + \tilde{n}(z,t)$ and $v = v_0(z) + \tilde{v}(z,t)$, where $\tilde{n}$ and $\tilde{v}$ are small perturbed quantities. The linearized governing equations are

$$\frac{1}{n_0}\frac{\partial \tilde{n}}{\partial t} + \frac{\partial \tilde{v}}{\partial z} + v_0 \tilde{Y} + \tilde{v}\frac{\partial_z n_0}{n_0} - \tilde{v}\frac{\partial_z B}{B} = 0 \tag{2.5}$$

$$\frac{\partial \tilde{v}}{\partial t} + \frac{\partial (v_0 \tilde{v})}{\partial z} = -\tilde{Y} \tag{2.6}$$

where

$$\tilde{Y} \equiv \frac{1}{n_0}\frac{\partial \tilde{n}}{\partial z} - \frac{\partial_z n_0}{n_0^2}\tilde{n} = \frac{\partial}{\partial z}\left(\frac{\tilde{n}}{n_0}\right)$$

2.3 Polynomial Eigenvalue Problem

In order to investigate the instability of magnetic nozzle, we need formulate it as an eigenvalue problem. To do that, we assume the perturbed density and velocity are oscillatory, i.e. $\tilde{n}, \tilde{v} \sim \exp(-i\omega t)$, where ω is the oscillation frequency of the perturbed quantities. This frequency can be a complex number. If $\omega = \omega_r + i\omega_i$, then the perturbed quantities becomes $\tilde{n} \sim \exp(\omega_i t)\exp(i\omega_r t)$, which means it grows exponentially with time.

Let $\tilde{n} \sim \exp(-i\omega t)$ and $\tilde{v} \sim \exp(-i\omega t)$, then we have the polynomial eigenvalue problem

$$\begin{aligned} &\omega^2 \tilde{v} \\ &+2i\omega\left(v_0\frac{\partial}{\partial z} + \frac{\partial v_0}{\partial z}\right)\tilde{v} \\ &+\left[(1-v_0^2)\frac{\partial^2}{\partial z^2} - \left(3v_0 + \frac{1}{v_0}\right)\frac{\partial v_0}{\partial z}\frac{\partial}{\partial z} - \left(1 - \frac{1}{v_0^2}\right)\left(\frac{\partial v_0}{\partial z}\right)^2 - \left(v_0 + \frac{1}{v_0}\right)\frac{\partial^2 v_0}{\partial z^2}\right]\tilde{v} = 0 \end{aligned} \tag{2.7}$$

Chapter 3

Methodology

3.1 Spectral Method

Spectral method is one of the best tools to solve PDE and ODE problems. [7] The central idea of spectral method is by discretizing the equation, we can transform that to a linear system or an eigenvalue problem.

Here we reformulate the polynomial eigenvalue problem, Eq.(2.7) as the following,

$$\begin{bmatrix} 0 & 1 \\ \hat{M} & \hat{N} \end{bmatrix} \begin{bmatrix} \tilde{v} \\ \omega\tilde{v} \end{bmatrix} = \omega \begin{bmatrix} \tilde{v} \\ \omega\tilde{v} \end{bmatrix} \tag{3.1}$$

where the operators $\hat{M}$ and $\hat{N}$ are defined as

$$\hat{M} = -\left[(1-v_0^2)\frac{\partial^2}{\partial z^2} - \left(3v_0 + \frac{1}{v_0}\right)\frac{\partial v_0}{\partial z}\frac{\partial}{\partial z} - \left(1 - \frac{1}{v_0^2}\right)\left(\frac{\partial v_0}{\partial z}\right)^2 - \left(v_0 + \frac{1}{v_0}\right)\frac{\partial^2 v_0}{\partial z^2}\right]$$
$$\hat{N} = -2i\left(v_0\frac{\partial}{\partial z} + \frac{\partial v_0}{\partial z}\right)$$

This becomes an ordinary algebraic eigenvalue problem if we discretize the operators and the function $\tilde{v}$. In this thesis, finite-difference, finite-element and spectral-element discretizations are used.

3.2 Shooting Method

Shooting method can be used to solve eigenvalue problem with specified boundary values,

$$g(\tilde{v}(z);\omega) = 0, \quad z_l \le z \le z_r, \quad \tilde{v}(z_l) = \tilde{v}_l, \tilde{v}(z_r) = \tilde{v}_r \tag{3.2}$$

where ω is the eigenvalue to be solved.

Suppose a eigenvalue problem can be formulated as

$$\frac{\mathrm{d}}{\mathrm{d}z}\mathbf{u} = \mathbf{f}(\mathbf{u}, z; \omega), \quad z_l < z < z_r, \quad \mathbf{u}(z_l) = \mathbf{u}_l$$

where $\mathbf{u} \in \mathbb{R}^2$. Fixed an ω, we can approximate $\mathbf{u}(z_r)$ by applying algorithms such as Runge-Kutta or Leap-frog.

Define F by $F(\mathbf{u}_l;\omega) = \tilde{v}(z_r;\omega)$. This function F takes in the initial value $\mathbf{u}_l$ and a fixed ω, and outputs the "landing point" $\tilde{v}(z_r;\omega)$. If ω is an eigenvalue of Eq.(3.2), then $\tilde{v}(z_r;\omega) = \tilde{v}_r$. Now we can find eigenvalues to Eq.(3.2) by solving the roots to the scalar equation

$$h(\omega) = F(\mathbf{u}_l;\omega) - \tilde{v}_r$$

Having this higher view of shooting method in mind, we first transform Eq.(2.7) to a IVP,

$$
\begin{aligned}
v' &= u \\
u' &= \frac{-1}{1-v_0^2}\left[\omega^2 v + 2i\omega(v_0 + v_0' v) - \left(3v_0 - \frac{1}{v_0}\right) v_0' u - \left(1 - \frac{1}{v_0}^2\right)(v_0')^2 v - \left(v_0 + \frac{1}{v_0} v_0'' v\right)\right]
\end{aligned}
$$

In order to get initially value for cases with transonic velocity profiles, we need to expand the solution at the singularity.

3.2.1 Expansion at Singularity

If the equilibrium velocity profile v_0 is a transonic profile, then $v_0(0) = 1$ at the throat of the magnetic mirror configuration. This is a singularity. More specifically, it is a regular singular point.

In order to supply initial values to shooting method, we need to expand Eq.(2.7) at the singularity,

$$
-2v_0'(0) z \frac{\partial^2 \tilde{v}}{\partial z^2} + (2i\omega - 4v_0'(0)) \frac{\partial \tilde{v}}{\partial z} + (\omega^2 + 2i\omega v_0'(0) - 2v_0''(0))\tilde{v} = 0
$$

Use Frobenius method, assuming $\tilde{v} = \sum_{n\geq 0} c_n z^{n+r}$, we get two different roots, $r = 0$ and $r = 1 - a$. They correspond to finite solution and diverging solution near the singularity, respectively. The coefficients of the power series are given by where

$$
\begin{aligned}
c_n &= \frac{(-1)^n b^n c_0}{\prod_{k=0}^{n-1}(n + r - k)(n + r - 1 + a - k)} \\
&= (-1)^n b^n c_0 \frac{\Gamma(r+1)\Gamma(r+a)}{\Gamma(n+r+1)\Gamma(n+r+a)}
\end{aligned}
$$

where

$$
a = \frac{2i\omega - 4v_0'(0)}{-2v_0'(0)}; \quad b = \frac{\omega^2 + 2i\omega v_0'(0) - 2v_0''(0)}{-2v_0'(0)}
$$

Worth to mention that the diverging solution goes like

$$
\tilde{v}(z) \sim z^{1-a} = z^{-1-\omega_i / v_0'(0)} z^{i\omega_r / v_0'(0)}
$$

where $\omega = \omega_r + i\omega_i$. Meaning that the solution will be divergent iff $\omega_i > -v'(0)$.

Now we have the initial conditions to the IVP,

$$
\begin{aligned}
v'(0) &= c_1 \\
u'(0) &= v''(0) = 2c_2
\end{aligned}
$$

Chapter 4

Numerical Experiments

4.1 Constant Velocity Case - Subsonic

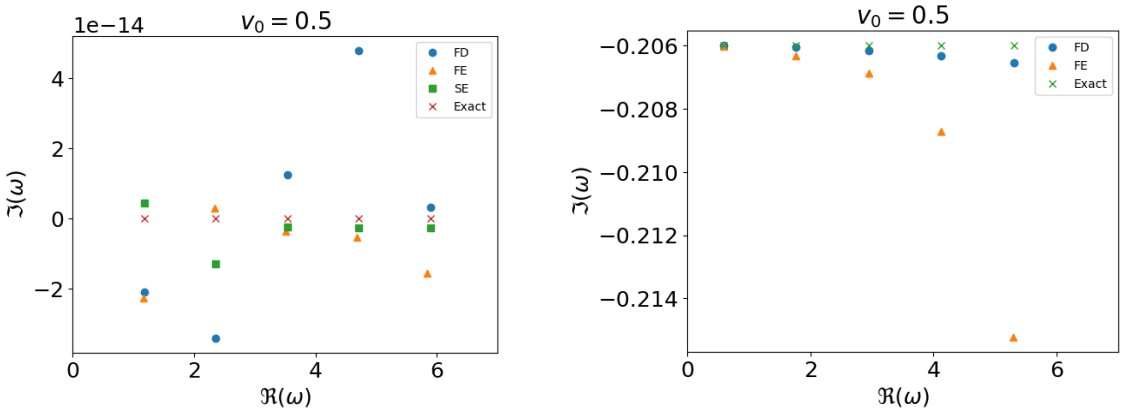

(a) Dirichlet boundary, all modes are stable.

(b) Fixed-open boundary, all modes are stable.

Figure 4.1: Showing the first 5 eigenvalues. In the Dirichlet boundary case, all methods are close to the exact eigenvalues. Meanwhile, finite-difference method has higher accuracy than finite-element method in fixed-open case.

4.2 Constant Velocity Case - Supersonic

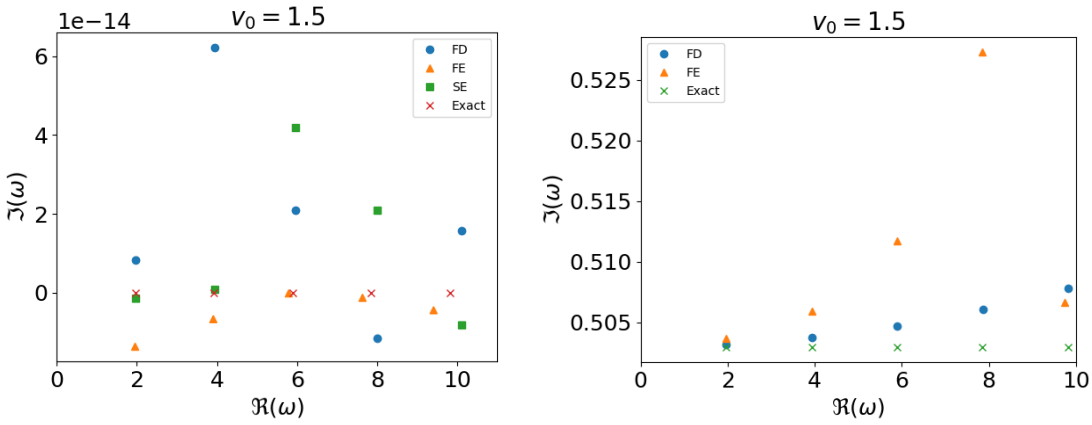

(a) Dirichlet boundary, filtered modes are stable. (b) Fixed-open boundary, all modes are unstable.

Figure 4.2: Showing the first 5 eigenvalues. In the Dirichlet boundary case, all methods are close to the exact eigenvalues. Meanwhile, finite-difference method has higher accuracy than finite-element method in fixed-open case.

4.3 Error

Because the existence of exact solution to problems Eq.(2.7). The case with constant velocity profile is used as a sanity check. It allows us to verify the correctness of each method's implementation. This also serves as a reference to the accuracy spectral methods can achieve.

From Fig.4.1 and Fig.4.2, we see that the order of growth rates is about 10^{-14} for both subsonic and supersonic cases if the boundary condition is Dirichlet. We will use it a reference to the accuracy of our numerical methods. If a method produces growth rates with order close to 10^{-14}, we consider the growth rates to be 0.

Table 4.1: Relative error of each eigenvalue.

$v_0 = 0.5$	1	2	3	4	5
FD	2.827e-05	1.130e-04	2.541e-04	4.512e-04	7.040e-04
FE	0.005	0.005	0.006	0.008	0.010
SE	2.896e-05	1.157e-04	2.603e-04	4.626e-04	7.217e-04

$v_0 = 1.5$	1	2	3	4	5
FD	0.001	0.005	0.010	0.019	0.030
FE	0.006	0.010	0.019	0.029	0.043
SE	0.001	0.005	0.011	0.019	0.030

Table 4.2: Relative error of each eigenvalue. Notice that the ground mode for subsonic case is non-zero.

$v_0 = 0.5$	0	1	2	3	4
FD	1.209e-05	3.458e-05	5.775e-05	8.153e-05	1.061e-04
FE	8.090e-05	2.007e-04	2.981e-04	6.596e-04	1.821e-03

$v_0 = 1.5$	1	2	3	4	5
FD	9.163e-05	2.435e-04	4.833e-04	8.160e-04	1.243e-03
FE	4.431e-04	7.924e-04	1.516e-03	3.103e-03	8.001e-03

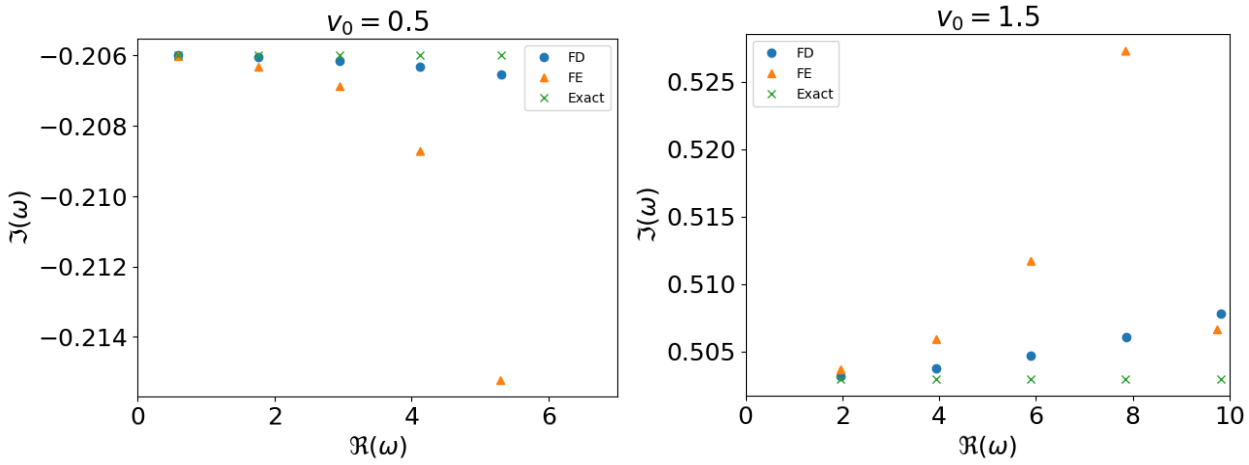

(a) All modes are stable.

(b) All modes are unstable.

Figure 4.3: Showing the first 5 eigenvalues of each method. Finite-difference method has much better accuracy than finite-element method.

4.4 Subsonic Case

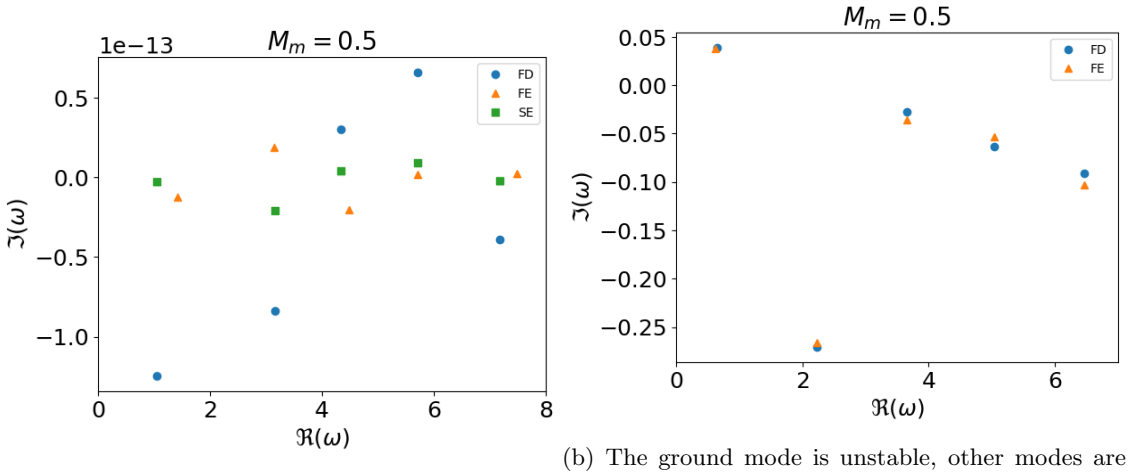

(a) Dirichlet boundary, all modes are stable.

(b) The ground mode is unstable, other modes are stable.

Figure 4.4: Showing the first 5 modes. It suggests that the subsonic flow in magnetic nozzle is stable.

4.5 Supersonic Case

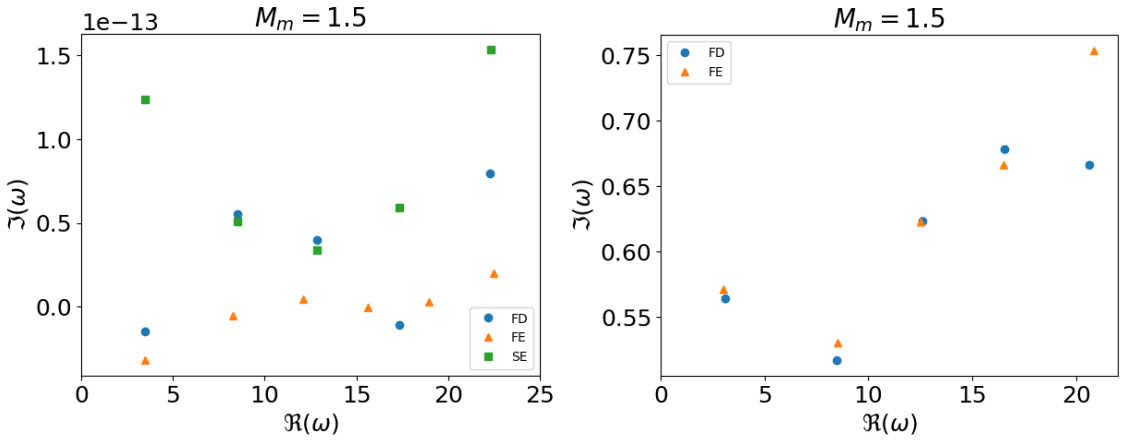

(a) Dirichlet boundary, filtered modes are stable. (b) Fixed-open boundary, all modes are unstable.

Figure 4.5: This suggests that the supersonic flow is stable if the boundary is Dirichlet and unstable if the boundary is left-fixed-right-open.

4.6 Accelerating Case

Starting from the singular point, we shoot the solution to the left boundary. We find the set of eigenvalues such that $\tilde{v}(-1) = 0$. With these eigenvalues, we can extend the solution to the supersonic region $(0, 1]$. The first five eigenvalues are drawn in the graph.

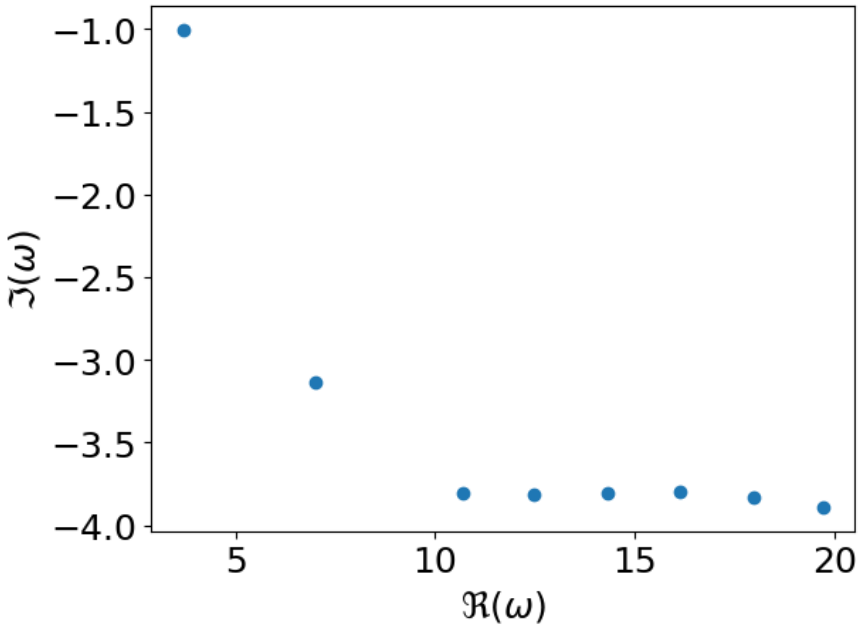

Figure 4.6: All modes are stable.

Chapter 5

Future Work

This research is still needs improvement. To improve the credibility of the results, different numerical calculation methods will be employed.

- Investigate and interpret the instability of an accelerating flow with non-zero left boundary. See Fig.5.1
- Setup a analytically solvable problem with similar configuration. Compare the analytical results to the the experimental computations to better understand the physics.

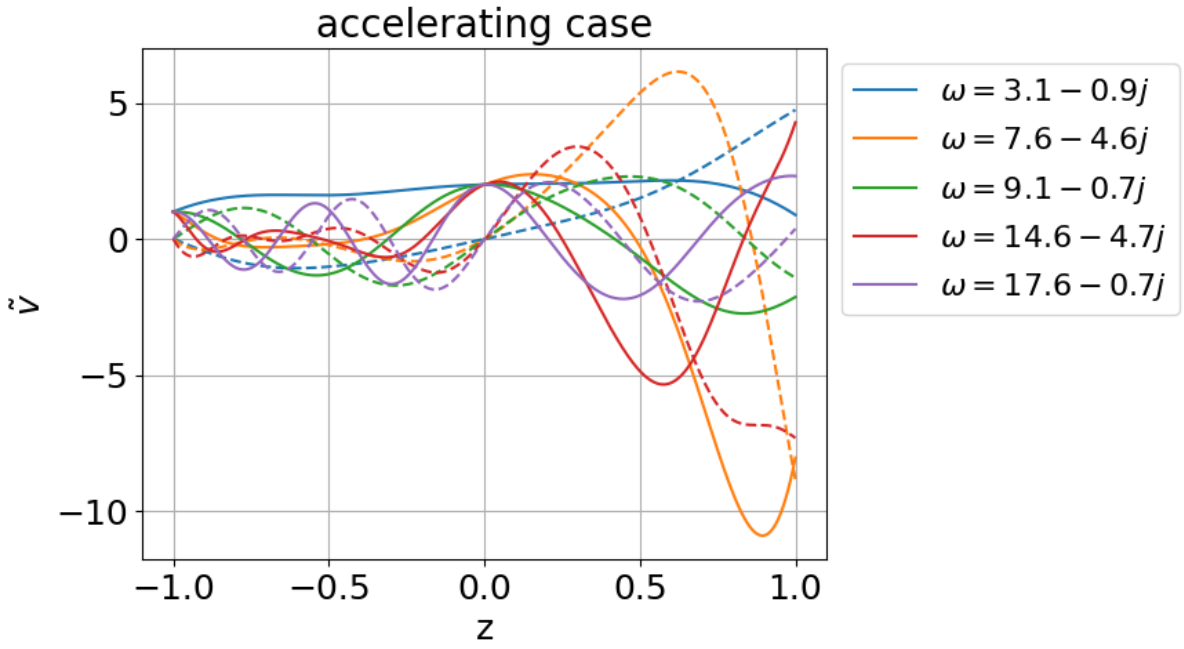

Figure 5.1: By matching the real part of the perturbation to a nonzero real value, we get different eigenvalues and eigenfunctions. What is the physical interpretation of "non-zero" boundary value? How do we interpret these eigenvalues?

Bibliography

[1] Toshiki Aikawa. The stability of spherically symmetric accretion flows. *Astrophys Space Sci*, 66(2):277–285, December 1979.

[2] H. Bondi. On Spherically Symmetrical Accretion. *Monthly Notices of the Royal Astronomical Society*, 112(2):195–204, April 1952.

[3] Francis F. Chen. *Introduction to Plasma Physics and Controlled Fusion*. Springer International Publishing, Cham, 2016.

[4] Klaus Jockers. On the stability of the solar wind. *Sol Phys*, 3(4):603–610, April 1968.

[5] Eric Keto. Stability and solution of the time-dependent Bondi–Parker flow. *Monthly Notices of the Royal Astronomical Society*, 493(2):2834–2840, April 2020.

[6] A. I. Smolyakov, A. Sabo, P. Yushmanov, and S. Putvinskii. On quasineutral plasma flow in the magnetic nozzle. *Physics of Plasmas*, 28(6):060701, June 2021.

[7] Lloyd N Trefethen. *Spectral Methods in Matlab*.